ChemComm

Chemical Communications

rsc.li/chemcomm

ROYAL SOCIETY
OF CHEMISTRY
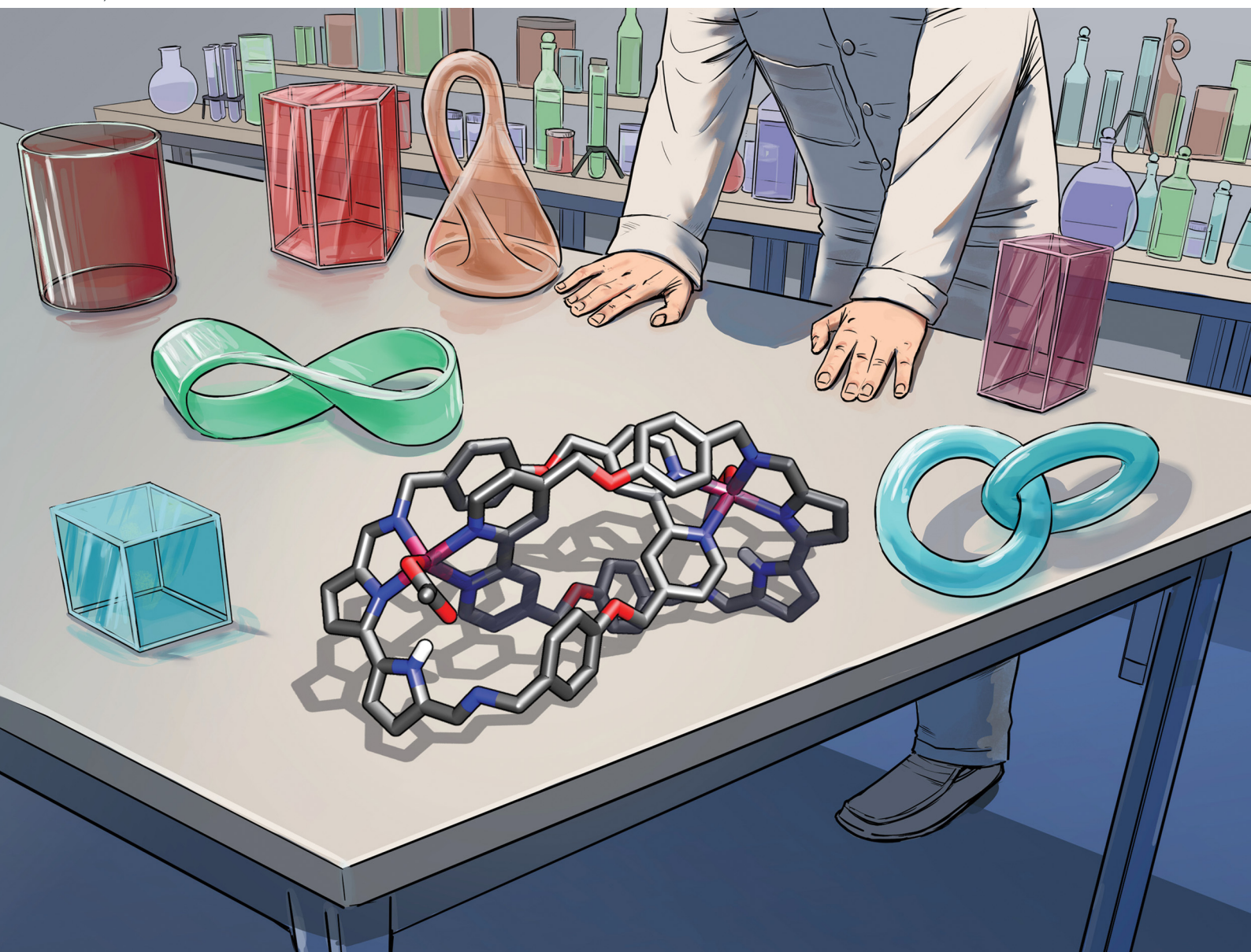
COMMUNICATION
Bartosz Szyszko *et al.*
Mechanically interlocked porphyrinoids: self-assembly of
metal-stabilised catenaphyrins

Check for updates

Mechanically interlocked porphyrinoids: self-assembly of metal-stabilised catenaphyrins

Aleksandra Sarwa, [ID] [a] Maksym Matviyishyn, [ID] [a] Jędrzej P. Perdek, [ID] [a] Bartosz Trzaskowski, [ID] [b] Dagmara Kulesza, [ID] [a] Eugeniusz Zych [ID] [a] and Bartosz Szyszko [ID] *[a]

Metal-stabilised catenanes comprising two porphyrinoid-like macrocycles were obtained *via* the self-assembly of bipyrrole and dipyrromethane dialdehydes with bipyridyl-based diamine in the presence of a metal template. Reported architectures exhibited conformational flexibility and distinct photophysical properties, with dipyrrin-based systems displaying strong luminescence.

Mechanically interlocked molecules (MIMs) containing tetra-pyrrolic macrocycles – especially porphyrins – have attracted considerable attention in supramolecular chemistry owing to their rich and versatile coordination chemistry and their ability to mediate charge and energy transfer processes.[1] The capacity of metalloporphyrins for axial coordination has been widely exploited to control molecular motion in artificial molecular machines.[2] This property has also enabled the development of porphyrin-based interlocked receptors in which the metal centre plays a decisive role in guest recognition.[3]

While MIMs incorporating porphyrins are well established, examples involving other pyrrolic macrocycles remain comparatively rare. Mechanically interlocked architectures based on porphyrinoids – macrocycles structurally related to archetypal oligopyrroles – are of special interest due to their distinctive properties, including versatile redox behaviour,[4] the ability to stabilise radical states,[5] absorption and emission across a broad spectral range,[6] unusual aromaticity,[7] and the reactivity it confers,[8] as well as conformational dynamics[9] and unique stereochemical features.[10] Contributions in this area so far include the use of macrocycles such as corroles,[11] calix[4]pyrroles,[12] calix[4]phyrins,[13,14] and their structural elements to construct rotaxanes and catenanes.[15–18]

Our group recently showed that diformylpyrrole undergoes self-assembly to afford topologically non-trivial architectures exhibiting conformational flexibility.[19] Here, we extend this approach to show that more elaborate, bipyrrole- and dipyrrin-based synthons can also be used to target Mechanically Interlocked Porphyrinoids (MIPs). The straightforward synthesis afforded M(II)-stabilised catenaphyrins, which exhibited intrinsic flexibility and distinctive emission in solution.

In our search for suitable porphyrinoid-derived structural motifs for the self-assembly of MIPs, we envisioned that imine derivatives of 2,2′-bipyrrole and dipyrrin would provide a reasonable basis for accessing new assemblies. These two motifs represent fundamental building blocks of both regular-sized, as well as contracted and expanded porphyrinoids. Although two imine synthons differ in conjugation and the charge they acquire upon deprotonation, they both belong to a class of formally tetradentate ligands that have been scarcely explored in self-assembly studies.[20] To assess the potential of the building blocks for the self-assembly of MIMs, we envisioned their combination with a bipyridine-based diamine **1**.[21] The latter has proven to be a highly versatile component, providing a variety of assemblies including catenanes, trefoil knots, and Solomon links, depending on the aldehyde partner and the metal cations employed to stabilise the resulting architectures.[19–23]

First, **1** was reacted with 5,5′-diformyl-2,2′-bipyrrole **2**, and zinc(II) acetate in *iso*-propanol in the presence of excess *N,N*-diisopropylethylamine (DIPEA, 72 equiv.) (Scheme 1). Refluxing the mixture for 1 hour gave a dark yellow solution. Precipitation of the crude product, followed by recrystallisation from chloroform/cyclohexane, afforded **3-Zn** in 16% yield. The clean formation of an analogous cadmium(II) assembly, **3-Cd** (11%), required reacting the components in chloroform.

The ESI-MS spectrum of **3-Zn** showed two signals at *m/z* 1341.3387 ([M−AcO]$^+$) and 641.1634 ([M−2(AcO)]$^{2+}$), consistent with the presence of two Zn(II) cations stabilising the structure (Fig. S38, SI). Similarly, the ESI-MS of **3-Cd** displayed a series of signals indicative of two cadmium(II) centres incorporated within the assembly, as further supported by the characteristic isotopic pattern (Fig. S43–S45, SI). Definitive evidence for the structure of the new assembly was obtained from X-ray diffraction (SCXRD) studies (Fig. 1). Single crystals of **3-Zn** suitable for analysis were grown by slow evaporation of a methanolic

[a] *Faculty of Chemistry, University of Wrocław, 14 F. Joliot-Curie St., 50-383 Wrocław, Poland. E-mail: bartosz.szyszko@uwr.edu.pl; Web: https://www.bszyszko.pl*
[b] *Centre of New Technologies, University of Warsaw, 2c Banach St., 02-097 Warsaw, Poland*
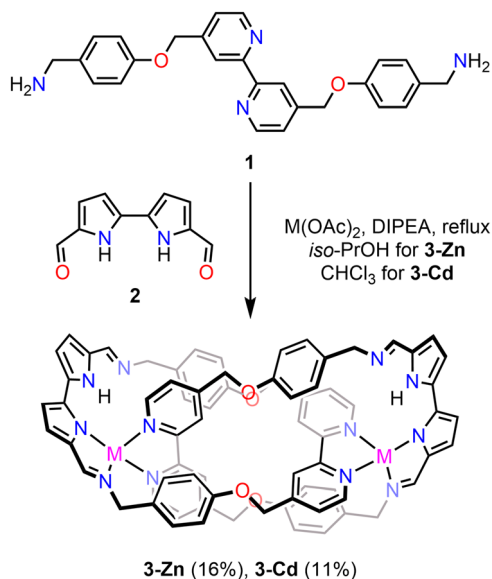
Scheme 1 Synthesis of **3-M**. Coordinating anions bound to M(II) were omitted for clarity.

solution of the assembly. The compound crystallised in the trigonal system, space group $P3_121$.

The molecular structure revealed that **3-Zn** is a [2]catenane composed of two identical macrocycles, each incorporating a diiminobipyrrole fragment and an amine-based component. The assembly is stabilised by two crystallographically equivalent zinc(II) cations. Each Zn(II) centre is coordinated to two bipyridine nitrogen atoms (dZn–N_{bpy}: 2.081(2), 2.188(3) Å) of one macrocyclic ring, as well as the imine nitrogen (dZn–N_{im}: 2.053(4) Å) and one pyrrolide (dZn–N_{pyrr}: 2.162(2) Å) of the bipyrrole subunit in the other macrocycle. The second pyrrolic nitrogen remains protonated. Each Zn(II) also binds an acetate anion (dZn–O1: 2.052(2) Å), compensating the overall charge of the complex. Both metal centres coordinated by five donor atoms acquired a distorted square-pyramidal geometry. The basal plane consisted of three nitrogen atoms and one oxygen, with the apical position occupied by the imine nitrogen donor. While the three nitrogens and Zn(II) remained almost in the same plane, the Zn–O bond deviated from it (dO1–N_3Zn: 1.435 Å), most likely due to the competitive hydrogen bonding between the second carboxylate oxygen and the bipyrrole N–H (dNH···O2: 1.97 Å).

In contrast to the molecular structure of **3-Zn** detected in the solid state, the ^1H NMR spectrum (CD$_3$OD, 300 K) displayed
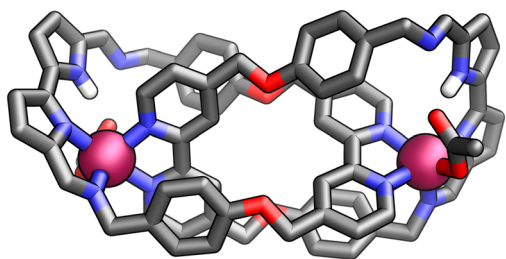

Fig. 1 The X-ray molecular structure of **3-Zn**. Apolar protons were omitted for clarity.
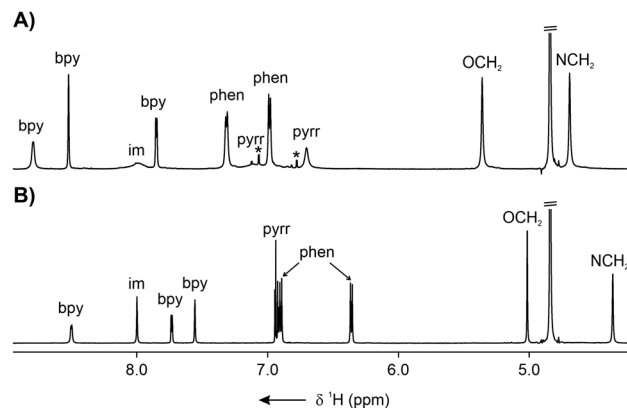

Fig. 2 The ^1H NMR spectra (CD$_3$OD, 300 K, 600 MHz) of (A) **3-Zn** and (B) **5-Zn**.

only ten resonances, suggesting a high effective symmetry of the assembly in solution (Fig. 2A and Fig. S2, SI). However, the pronounced broadening of several signals indicated that this is likely a result of a dynamic process averaging the catenane structure at 300 K.[19,20] The bipyridyl signals were identified at 8.79, 8.52, and 7.85 ppm, whereas the two broad β-pyrrolic resonances appeared at 7.04 and 6.70 ppm. The phenylene signals were observed at 7.31 and 6.98 ppm, followed by the OCH$_2$ and NCH$_2$ lines at 5.36 and 4.69 ppm, respectively.

The ^1H NMR linewidths of **3-Zn** exhibited a pronounced temperature dependence (Fig. S3, SI). Gradual broadening of the signals was observed upon cooling from 330 to 180 K, but their decoalescence was not detected even at low temperature. Thus it is anticipated that in the solution **3-Zn** acquires a higher symmetry than in the solid state, or that the dynamic process it is involved in has a high rate constant. Nevertheless, recording the low-temperature spectrum enabled the identification of one of the two β-pyrrolic resonances and the imine signal, both of which were markedly broadened at 300 K. In contrast, for **3-Cd**, the multiplication of the number of signals became apparent below 240 K; however, sharp resonances were not observed even at low temperatures (Fig. S14, SI). Peculiarly, whereas in diiminopyrrole-based assemblies the dynamic process effectively involved the breaking and reformation of one of the two imine nitrogen–metal bonds, in the case of bipyrrole-containing species, such a transformation would necessarily be accompanied by a concomitant proton-transfer process engaging the pyrrolide and the pyrrole ring not involved in metal coordination. The analysis of a hypothetical transformation wherein the Zn(II) and proton were swapped between two pyrroles of bipyrrole was carried out employing semiempirical calculations (Fig. S59 and S60, SI). The estimated energy barriers for such processes were found to be 56 kcal mol^{-1} for **3-Zn** and 45 kcal mol^{-1} for **3-Cd**, rendering them highly unlikely (see SI). Thus, it is anticipated that the dynamic event is more intricate, requiring the involvement of acetate(s) in the proton transfer step(s), or tautomerisation employing the bipyrrole unit and sidearm imine group(s) in the organic ligand.[24]

Once the principles governing the self-assembly of **1** and **2** were established, the next step was the construction of dipyrrin-incorporated catenaphyrins **5-M** (Scheme 2). To access the
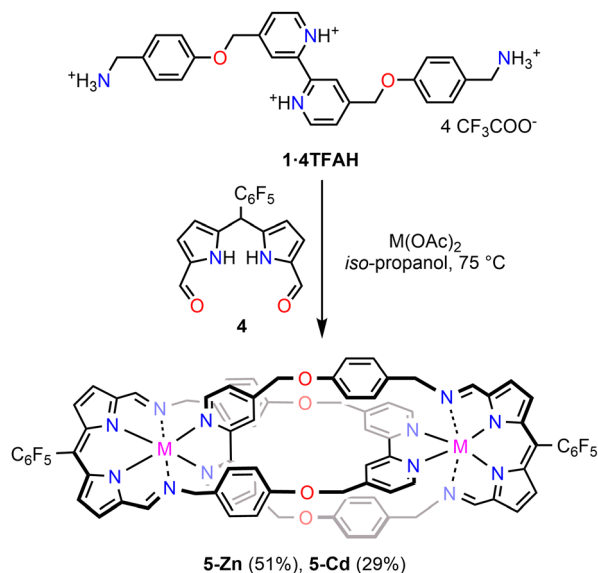
Scheme 2 Synthesis of **5-M**. Anions coordinated to M(II) were omitted for clarity.

desired architecture, *meso*-pentafluorophenyl diformyldipyrromethane **4** was employed as a key precursor. It has been shown that, upon metalation, dipyrromethanes readily undergo spontaneous oxidation to the corresponding dipyrrin species.[25] This was expected to be further enhanced by the presence of a pentafluorophenyl group in the *meso*-position.[26–28] Thus, the reaction of amine tetrakis(trifluoroacetate) **1·4TFAH** was carried out with **4** and zinc(II) or cadmium(II) acetates in *iso*-propanol at 75 °C. After post-synthetic workup, a single product, *i.e.*, binuclear Zn(II) or Cd(II)-stabilised [2]catenaphyrin **5-M** was isolated in 51, and 29% yield, respectively.

The identity of the assemblies was confirmed by a combination of mass spectrometry and extensive NMR spectroscopic analyses (Fig. S17–S37 and S46–S51, SI). The ESI-MS spectrum of **5-Zn** displayed two signals at m/z 1751.2713 (M–TFA)$^+$ and 819.1425 (M–2TFA)$^{2+}$, consistent with the incorporation of two Zn(II) cations within the assembly (Fig. S46, SI). The presence of two metal centres was further corroborated by comparing the experimental and simulated isotopic patterns for **5-Cd** (Fig. S49–S51, SI).

All attempts to obtain SCXRD-quality crystals of **5-M** were unsuccessful, resulting in the formation of Zn(II)/Cd(II) complexes of a dipyrrin acetal (Fig. S58, SI). Consequently, the geometry of **5-Zn** and **5-Cd** was optimised at the DFT-B3PW91 level of theory with the LanL2DZ basis set for metal cations, including methanol solvation modelled by the PCM approach (see SI for details). In the case of **5-Zn**, the two most favourable conformers displayed nearly identical energies (within 0.1 kcal mol^{-1}) and geometries (RMSD < 0.01 Å), with Zn(II) coordinated by both bipyridyl nitrogen atoms, two dipyrrin nitrogen atoms, and oxygen of the acetate (Fig. S61, SI). In each coordination pocket, one imine nitrogen was directed towards Zn(II), approaching a Zn–N$_{im}$ distance of 2.63 Å, while the other pointed outwards, preventing metal binding. The optimised geometry appeared viable and exhibited features similar to those of **3-M** and iminophenanthroline-comprising [2]catenanes.[20] For **5-Cd**,

two of the three low-energy conformers showed analogous geometrical features, while the third featured both imine nitrogens oriented towards the catenane cavity (Fig. S62, SI).

The ^{1}H NMR spectrum of **5-M** (CD$_3$OD, 300 K) revealed, similar to **3-M**, signals corresponding to a high effective symmetry species in solution (Fig. 2 and Fig. S17, S30, SI). For **5-Zn**, a single imine resonance was observed at 8.00 ppm, accompanied by three bipyridine signals at 8.50, 7.73, and 7.56 ppm. Multiplets of the phenyl rings appeared at 6.90 and 6.36 ppm, while the β-pyrrolic protons resonated at 6.94 and 6.92 ppm. The absence of the *meso*-H signal indicated that dipyrromethane underwent spontaneous oxidation to dipyrrin during self-assembly. Upon lowering the temperature from 300 to 180 K, a gradual desymmetrisation was detected (Fig. S18, SI), consistent with the dynamic stereoisomerisation.[19,20]

The 1 ns molecular dynamics study was performed to investigate **5-M** flexibility at 300 K. Interestingly, immediately after the initiation of the simulation, metal cations shifted from a position closer to one pyrrole–imine moiety towards a more symmetrical arrangement, interacting with both pyrroles, even though geometry optimisation clearly indicated a preference for lower symmetry geometries (Fig. S63 and Animation S1, S2, SI). The M–N$_{im}$ bonds cleavage and reforming was also detected, validating a plausible mechanism of the dynamic process.

With **3-M** and **5-M** in hand, their photophysical properties were evaluated. This seemed noteworthy, as the optical properties and luminescence of assemblies incorporating coordination motifs other than BODIPY dyes have received relatively little attention.[29] The often weak fluorescence of dipyrrin–metal complexes has limited their applications; however, recent advances in coordinative self-assembly have expanded their use for the construction of functional supramolecular architectures.

The bipyrrole- and dipyrrin-based catenaphyrins exhibited markedly different optical properties (Fig. 3). When dissolved in methanol, **3-Zn** produced yellow-orange solutions. Its UV-vis absorption spectrum displayed a series of low-intensity bands (log ε 1.4–1.7) between 250 and 320 nm, followed by broad absorptions centred around 350, 446, and 469 nm. In contrast, the presence of a conjugated dipyrrin unit in **5-Zn** resulted in intensely pink-violet solutions. The UV-vis absorption spectrum of **5-Zn** displayed four distinct bands with maxima at 290 (log ε = 4.9), 487 (a weak shoulder), 525 (4.6), and 562 nm (5.1). The emission spectrum of **5-Zn**, observed in the orange-red region, consisted of two overlapping components peaking around 580 and 620 nm (shoulder) upon excitation at 562 nm (Φ = 0.54). Similar spectroscopic features were observed for **5-Cd** (Fig. S54, SI). Time-dependent DFT (TD-DFT) calculations indicated that the fluorescence in **5-M** arises from a π*–π transition. Both the ground and excited states involved in this transition were primarily localised on pyrrole rings, with an additional contribution from the bridging *meso*-phenyl (Fig. S67 and S68, SI). This was further supported by the lack of low-lying metal-centred states in the Zn(II) cation, whose 3d^{10} configuration makes it photophysically inactive and maintains ligand-centred emission.

In summary, the use of pyrrole-based building blocks commonly employed in the synthesis of porphyrinoids, *i.e.*, dialdehydes
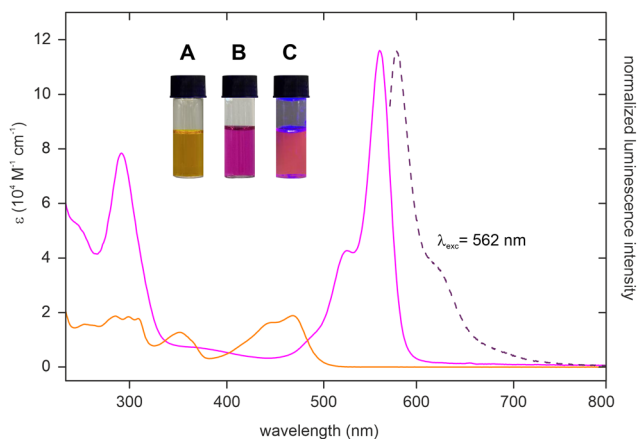
Fig. 3 UV-vis absorption spectra of **3-Zn** (orange solid line) and **5-Zn** (violet solid line) in CH$_3$OH at 298 K. The dotted line shows the fluorescence spectrum of **5-Zn** in CH$_3$OH recorded upon excitation at 562 nm at 298 K. The inset shows the colour of methanolic solutions of (A) **3-Zn**, (B) **5-Zn**, and (C) **5-Zn** under UV light (365 nm).

incorporating 2,2′-bipyrrole and dipyrrin scaffolds, enabled the selective formation of [2]catenanes through imine-based self-assembly in the presence of zinc(II) and cadmium(II) templates. These compounds were the sole products formed under the optimised conditions. The Hopf link topologies were confirmed by SCXRD, NMR spectroscopy, and mass spectrometry. The bipyrrole- and dipyrrin-derived catenanes exhibited notably different optical properties in solution, with **5-M** displaying efficient luminescence.

This work establishes an approach to constructing supramolecular architectures based on porphyrinoid structural motifs. It is believed that the synthetic accessibility of porphyrinoid-like interlocked assemblies opens the way to complex structures whose reactivity, dynamics, or optical properties are governed by the principal coordination motif. Further efforts in this direction will enable the development of increasingly sophisticated interlocked systems, including molecular knots incorporating pyrrole-based elements, *i.e.*, knotaphyrins, thereby further blurring the boundaries between MIMs and porphyrinoid chemistry.[30–32]

Conflicts of interest

There are no conflicts to declare.

Data availability

The data supporting this article have been included as part of the supplementary information (SI). Supplementary information is available. See DOI: https://doi.org/10.1039/d5cc05702g.

CCDC 2483444 and 2483443 contain the supplementary crystallographic data for this paper.[33a,b]

Notes and references

1 J. A. Faiz, V. Heitz and J.-P. Sauvage, *Chem. Soc. Rev.*, 2009, **38**, 422–442.
2 J. T. Wilmore, Y. Cheong Tse, A. Docker, C. Whitehead, C. K. Williams and P. D. Beer, *Chem. – Eur. J.*, 2023, **29**, e202300608.
3 J. T. Wilmore, A. Docker and P. D. Beer, *Dalton Trans.*, 2025, **54**, 1425–1432.
4 T. Ma, Z. Pan, L. Miao, C. Chen, M. Han, Z. Shang and J. Chen, *Angew. Chem., Int. Ed.*, 2018, **57**, 3158–3162.
5 T. Koide, G. Kashiwazaki, M. Suzuki, K. Furukawa, M. Yoon, S. Cho, D. Kim and A. Osuka, *Angew. Chem., Int. Ed.*, 2008, **47**, 9661–9665.
6 T. Tanaka, N. Aratani, J. M. Lim, K. S. Kim, D. Kim and A. Osuka, *Chem. Sci.*, 2011, **2**, 1414–1418.
7 M. Stępień, N. Sprutta and L. Latos-Grażyński, *Angew. Chem., Int. Ed.*, 2011, **50**, 4288–4340.
8 B. Szyszko and L. Latos-Grażyński, *Chem. Soc. Rev.*, 2015, **44**, 3588–3616.
9 B. Szyszko, M. J. Białek, E. Pacholska-Dudziak and L. Latos-Grażyński, *Chem. Rev.*, 2017, **117**, 2839–2909.
10 S. A. Balahoju, Y. K. Maurya, P. J. Chmielewski, T. Lis, M. Kondratowicz, J. Cybińska and M. Stępień, *Angew. Chem., Int. Ed.*, 2022, **61**, e202200781.
11 T. H. Ngo, J. Labuta, G. N. Lim, W. A. Webre, F. D'Souza, P. A. Karr, J. E. M. Lewis, J. P. Hill, K. Ariga and S. M. Goldup, *Chem. Sci.*, 2017, **8**, 6679–6685.
12 J. R. Romero, G. Aragay and P. Ballester, *Chem. Sci.*, 2017, **8**, 491–498.
13 R. A. Grzelczak, T. Basak, B. Trzaskowski, V. Kinzhybalo and B. Szyszko, *Angew. Chem., Int. Ed.*, 2025, **64**, e202413579.
14 R. A. Grzelczak, J. P. Perdek, M. Siczek, P. J. Chmielewski and B. Szyszko, *Org. Lett.*, 2025, **27**, 6310–6315.
15 B. Nisanci, S. Sahinoglu, E. Tuner, M. Arik, İ. Kani, A. Dastan and Ö. A. Bozdemir, *Chem. Commun.*, 2017, **53**, 12418–12421.
16 A. Andrievsky, F. Ahuis, J. L. Sessler, F. Vögtle, D. Gudat and M. Moini, *J. Am. Chem. Soc.*, 1998, **120**, 9712–9713.
17 M. Hicguet, L. Verrieux, O. Mongin, T. Roisnel, F. Berrée, A. Fihey, B. Le Guennic and Y. Trolez, *Angew. Chem., Int. Ed.*, 2024, **63**, e202318297.
18 T. Nakamura, G. Yamaguchi and T. Nabeshima, *Angew. Chem., Int. Ed.*, 2016, **55**, 9606–9609.
19 A. Sarwa, A. Białońska, M. Sobieraj, J. P. Martínez, B. Trzaskowski and B. Szyszko, *Angew. Chem., Int. Ed.*, 2024, **63**, e202316489.
20 T. Prakasam, M. Lusi, E. Nauha, J.-C. Olsen, M. Sy, C. Platas-Iglesias, L. J. Charbonnière and A. Trabolsi, *Chem. Commun.*, 2015, **51**, 5840–5843.
21 T. Prakasam, M. Lusi, M. Elhabiri, C. Platas-Iglesias, J.-C. Olsen, Z. Asfari, S. Cianférani-Sanglier, F. Debaene, L. J. Charbonnière and A. Trabolsi, *Angew. Chem., Int. Ed.*, 2013, **52**, 9956–9960.
22 R. A. Bilbeisi, T. Prakasam, M. Lusi, R. El Khoury, C. Platas-Iglesias, L. J. Charbonnière, J.-C. Olsen, M. Elhabiri and A. Trabolsi, *Chem. Sci.*, 2016, **7**, 2524–2531.
23 A. Sarwa, A. Khmara, K. A. Konieczny, D. Kulesza, E. Zych, B. Trzaskowski and B. Szyszko, *Angew. Chem., Int. Ed.*, 2025, **64**, e202423962.
24 E. M. Matson, J. A. Bertke and A. R. Fout, *Inorg. Chem.*, 2014, **53**, 4450–4458.
25 C. Brückner, V. Karunaratne, S. J. Rettig and D. Dolphin, *Can. J. Chem.*, 1996, **74**, 2182–2193.
26 M. Matviyishyn, A. Białońska and B. Szyszko, *Angew. Chem., Int. Ed.*, 2022, **61**, e202211671.
27 J. R. Pankhurst, T. Cadenbach, D. Betz, C. Finn and J. B. Love, *Dalton Trans.*, 2015, **44**, 2066–2070.
28 M. Matviyishyn, K. A. Konieczny, B. Trzaskowski and B. Szyszko, *Chem. – Eur. J.*, 2024, **30**, e202402932.
29 A. Loudet and K. Burgess, *Chem. Rev.*, 2007, **107**, 4891–4932.
30 Z.-H. Zhang, H.-N. Feng, G. Chi, D. A. Leigh and L. Zhang, *CCS Chem.*, 2023, **5**, 2448–2465.
31 W. Wang, S. Zhou, X. Yu, Q.-H. Guo, Y. Ma, J. Song, L. Zhang, X. Yan, L. Han, Q. Liao, X. Li, W.-B. Zhang, Y. Mai, S. Zhang, S. Che, H.-B. Yang, X. Fu and M.-X. Wang, *CCS Chem.*, 2024, **6**, 2084–2109.
32 G. Gil-Ramírez, D. A. Leigh and A. J. Stephens, *Angew. Chem., Int. Ed.*, 2015, **54**, 6110–6150.
33 (*a*) CCDC 2483444: Experimental Crystal Structure Determination, 2025, DOI: 10.5517/ccdc.csd.cc2pc73f; (*b*) CCDC 2483443: Experimental Crystal Structure Determination, 2025, DOI: 10.5517/ccdc.csd.cc2pc72d.